JOINT INSTITUTE FOR NUCLEAR RESEARCH
Dzhelepov Laboratory of Nuclear Problems

FINAL REPORT ON THE SUMMER STUDENT PROGRAM

Monte Carlo calculation of dose rate distributions in a SPECT-CT system. Modeling of SPECT phantom using GEANT4.

Supervisors:
Dr. Antonio Leyva Fabelo
MsC. Vladislav Rozhkov

Student:
Jorge Luis Valdes Albuernes,
InSTEC, Havana University,
Cuba

Participation period:
July 04 – September 28

Dubna, 2019

Abstract

The MCNPX and Geant4 radiation transport simulation codes have been used to study the dose rate distribution in a SPECT-CT scanner system for two types of photon sources, and to obtain the image that a semiconductor detector is capable of registering from a SPECT phantom when a coded aperture mask is used. The comparison between the results of both codes showed that the maximum difference between them was less than 10%, although on average this was 5%. In the text are presented and compared the calculated results of the minimum distances considered safe from the point of view of radiation protection for occupationally exposed personnel for different geometric conditions and types of radiation sources. The results when is introduced into the system a complementary Al and Pb wall protection are also presented and analyzed. An evaluation of the image registered by a CdTe detector of a SPECT phantom loaded with ^{99m}Tc and located at different angles with respect to the detector is performed.

Table of contents.

Contents

Introduction.

Each new technology, specifically mention those related to health and medicine, before putting it into operation requires a large number of tests and trials that ensure that when used they are as harmless as possible to man. This refers to both the patient and the staff that uses it.

All these tests are carried out from the moment the technique is conceived, while the construction work is being carried out, and after completion before being exploited.

Especially important are those diagnostic and medical treatment techniques that use ionizing radiation, which can be from simple and common X-ray equipment to sophisticated gamma cameras or PET and SPECT scanners.

In these studies, the mathematical modeling of radiation transport plays an important role because with its use it is possible to carry out the simulation experiments in the most real way possible and allows to calculate with great precision not only the doses distribution, but also some hard to measure quantities [1-3].

This work is carried out within the framework of a joint Russian-Cuban scientific project at the Dzhelepov Nuclear Problems Laboratory of JINR, where a scientific group of both countries with experience in working with computed tomography (CT) and the development, characterization, and introduction of advanced radiation detectors, work on the creation of a new preclinical SPECT-CT scanner based on an advanced hybrid semiconducting detector.

The current report has two parts:

Firstly, the calculation of the distribution with the distance of the dose rate for different geometries and sources in the vicinity of a SPECT-CT type scanner system was performed. The main objective is to determine the working distance considered safe for occupationally exposed personnel. The based-on Monte Carlo method code systems MCNPX and Geant4 were used for this.

Secondly, the response of a CdTe radiation detector to a a phantom for contrast and resolution evaluation is studied. The Geant4 software was used to perform this work.

The SPECT-CT tomography.

The term “computed tomography”, or CT, refers to a computerized X-ray imaging procedure in which a narrow beam of X-rays is aimed at a patient and quickly rotated around the body, producing signals that are processed by the machine’s computer to generate cross-sectional images, or “slices”, of the body [4]. These slices are called tomographic images and contain more detailed information than conventional X-rays. Once several successive slices are collected by the machine’s computer, they can be digitally “stacked” together to form a three-dimensional image of the patient that allows for easier identification and location of basic structures as well as possible tumors or abnormalities.

Although new and more refined imaging techniques have emerged after the CT, such as MRI ("Magnetic Resonance Imaging"), SPECT ("Single Photon Emission Computed Tomography") and PET ("Positron Emission Tomography "), CT remains the most widely used. The new combination of CT with other techniques has produced a new generation of equipment known as hybrid scanners, a new paradigm in obtaining medical and scientific images able to merge the obtained anatomical information with the functional.

Among these hybrid techniques, SPECT-CT stands out, combining SPECT tomography and computed tomography into one imaging system.

Recall that the SPECT tomography is a 3D nuclear medicine tomographic imaging technique using gamma rays [5]. The technique requires delivery of a gamma-emitting radioisotope (a radionuclide) into the patient, usually through injection into the bloodstream. On occasion, the radioisotope is a pure soluble dissolved ion. Most of the time, though, a marker radioisotope is attached to a specific ligand to create a radioligand, whose properties bind it to certain types of tissues. This marriage allows the combination of ligand and radiopharmaceutical to be carried and bound to a place of interest in the body, where the ligand concentration is seen by a gamma camera.

The SPCT-CT combination has many advantages that are reported in the literature, for example in [6-8].

MCNPX and GEANT4 code systems.

With the great development that technologies and especially computing have had, doors have been opened to the elaboration of increasingly realistic calculation codes for particle

transport simulation using the Monte Carlo method [9]. Of these softwares, two of the most used are the MCNP and MCNPX: "Monte Carlo N - Particle", and the GEANT-4: "GEometry ANd Tracking". The simulation scheme of particle transport is, more or less, similar in both codes, and the differences between them focus on the approximations or models used to describe the interactions and their greater or lesser flexibility when interacting with the user.

The MCNPX is a 3D code consisting of a group of subroutines for sequential simulation by the Monte Carlo Method [10] of the individual probabilistic events that make up the transport processes of 34 types of different particles and photons, in a geometric configuration given three-dimensional and with a varied composition of materials. This software has many applications some include radiological protection and dosimetry, radiological shielding, radiography, medical physics, nuclear criticality safety, detector design and analysis, etc.

Written in Fortran, it is fundamentally based on the use of the effective section of each type of interaction and the statistical nature of the transport process to predict the probability of distribution of specific parameters such as energy losses and angular detection.

To interact with the code, the user must create a file (input file) with all the information required to perform the simulation. The MCNPX input file contains the specifications of the materials that will be involved in the interaction process, the geometry of the experiment, the characteristics of the source and the outputs desired by the user (Tally). During the simulation of the interactions, the program will take into account all the specifications entered by the user in the input file. All the outputs used from the MCNPX are normalized by the number of incident particles from the source (or the number of stories calculated) and are reported together with their estimated relative error.

The GEANT4 code is a general-purpose Monte Carlo; it was developed for the needs of high-energy physics and applications at the CERN (European Organization for Nuclear Research) accelerator. It is written in C ++. This code system provides a complete set of tools for all detector simulation areas: geometry, tracking, detector response, run, event and tracking control, display and interface. The multidisciplinary nature of this code requires an abundant base of physical processes to control the various interactions of particles with the matter in a wide range of energy, from 250 eV to 1 TeV. For different physical processes there is the option to choose between different models. Its areas of application include high energy, nuclear and accelerator physics, space science and medicine. See more information in [11, 12].

In current work these two code systems were used to simulate the transport of X-rays, gamma and electrons in a SPECT-CT scanner in order to determine the distribution of the dose rate, and also to preliminary evaluate the detector response to the emission of a specific phantom loaded with ^{99m}Tc. In the first task the MCNPX was the main tool, while the GEANT4 was used only to verify the reliability of the results of the first. In the second task, only the GEANT4 software was employed.

Dose rate calculations in SPECT-CT system.

For the evaluation of the dose rate distribution at different points around the SPECT-CT system, some geometric considerations were taken into account.

In the case of SPECT configuration, a point source with photons isotropic emission was considered. It is positioned in the center of mouse phantom, inside of a sphere simulating the heart and emitting with energy 140 keV (^{99m}Tc). The activity of the source is 10 MBq.

For the CT configuration, the W anode X-ray tube was approximated to a point source positioned 1 mm in front of the anode. This source emits only in the phantom direction within a solid angle 20^{o}. The full X-ray tube energy spectrum was considered in the simulation and it was calculated using interpolating polynomials (TASMIP) for 120 keV (figure 1) [13].

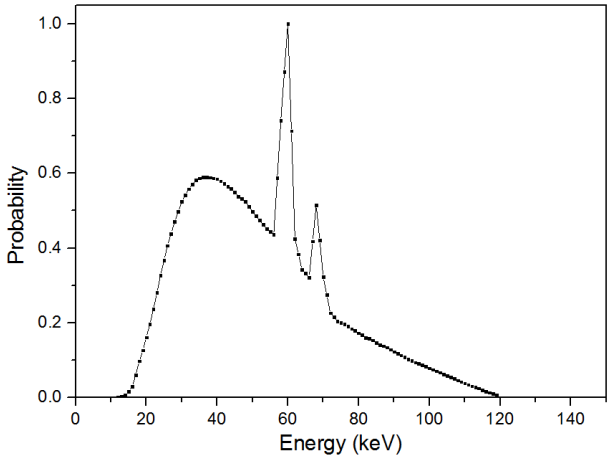

Figure 1. The tungsten anode spectrum with 1 keV intervals.

For the conversion of the outputs obtained by the code system from flow units to dose units, were used the coefficients recommended by [14]. For the selection of the correct coefficients, the rotation geometry was chosen (ROT). This is defined as the rotation of the irradiated body at uniform speed around the axis that passes through its center while this is irradiated by a beam that perpendicularly affects the phantom.

The geometry of the SPECT-CT arrangement is shown in figure 2. The image presented in (a) was taken from the visual environment of Geant4 and shows a general three-dimensional view of the system. In (b) the main parts of the simulated system are shown and identified.

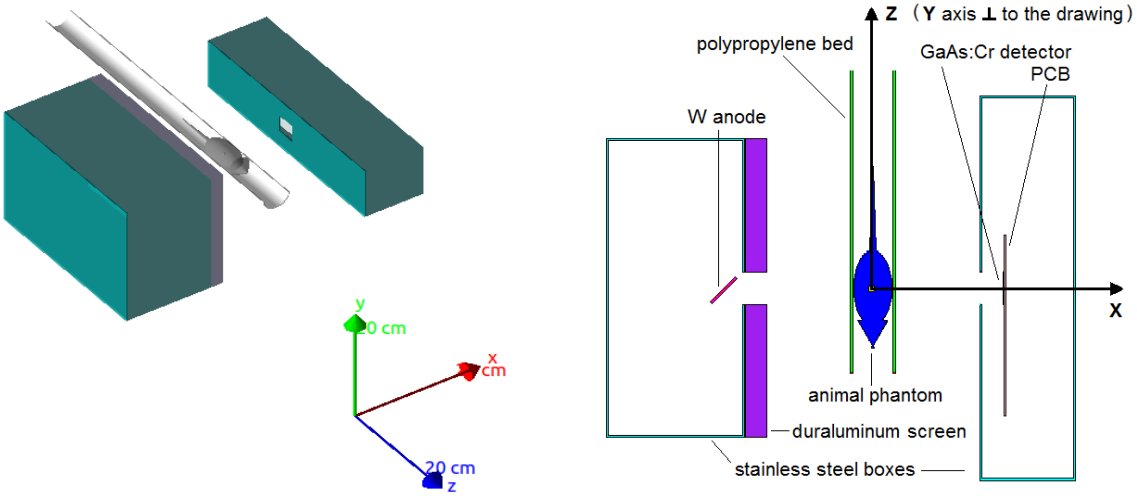

(a) (b)

Figure 2. 3D representation of the simulated geometry (a), and the respective diagram with the identification of the parts (b).

In the simulations, only the phantom, the bed, the X- ray or gamma source and the detector (hybrid 900 µm thick GaAs:Cr) were taken into account. Both, the source and detector were placed inside stainless steel boxes with windows for exit and entry of radiation. In front of the box where the X-ray source is positioned, an additional duraluminum protection is fixed. All materials and dimensions were chosen closest to the real MARS-CT system available in the Laboratory (figure 3).

Figure 3: MARS-CT micro scanner in the DLNP - JINR.

To illustrate the idea of both radiation sources in this SPECT-CT system, figure 4 presents a view of the simulated trajectories of the photons and electrons, (a) for the SPECT source with the energy 140 keV (^{99m}Tc) and (b) for the CT source with the W anode X-ray “tube”.

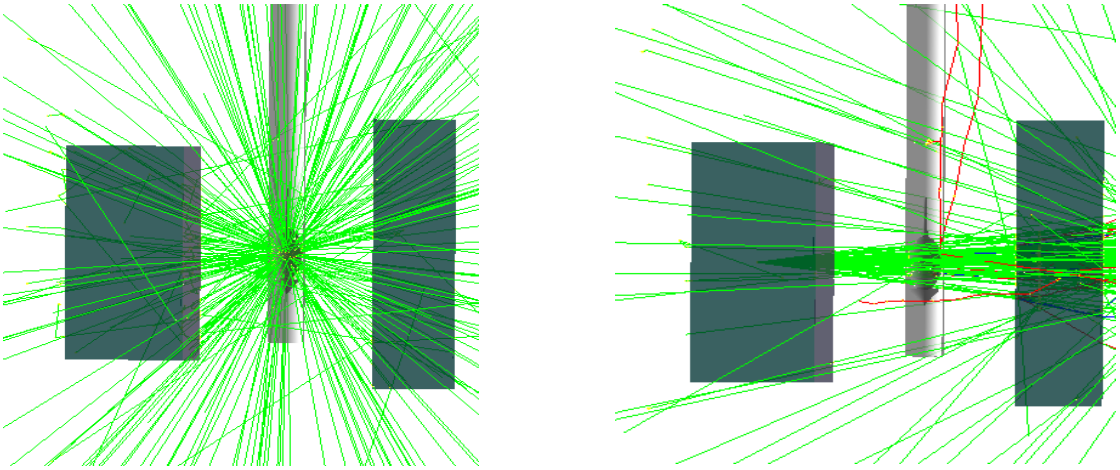

(a) (b)

Figure 4. Illustration of the tracks for photons (green lines) and secondary electrons (red lines) for SPECT-CT system in the case of ^{99m}Tc (a) and X-ray tube sources (b).

The errors of the calculations were always less than 5 %; this was accomplished using a high number of stories ($1x10^8$) for each run.

For professionals, - persons who are exposed to radiation from technical sources and are under dose surveillance, e.g. medical personnel or workers in a nuclear installation wearing a personal dosimeter - a whole-body dose rate of 20 mSv/year is permitted, and about 2.3 µSv/hour considered safe [14]. In all the figures below that show the simulation data, to facilitate the comparison, the dose rate value considered safe (2.3 µSv/hour) has been drawn with a red line.

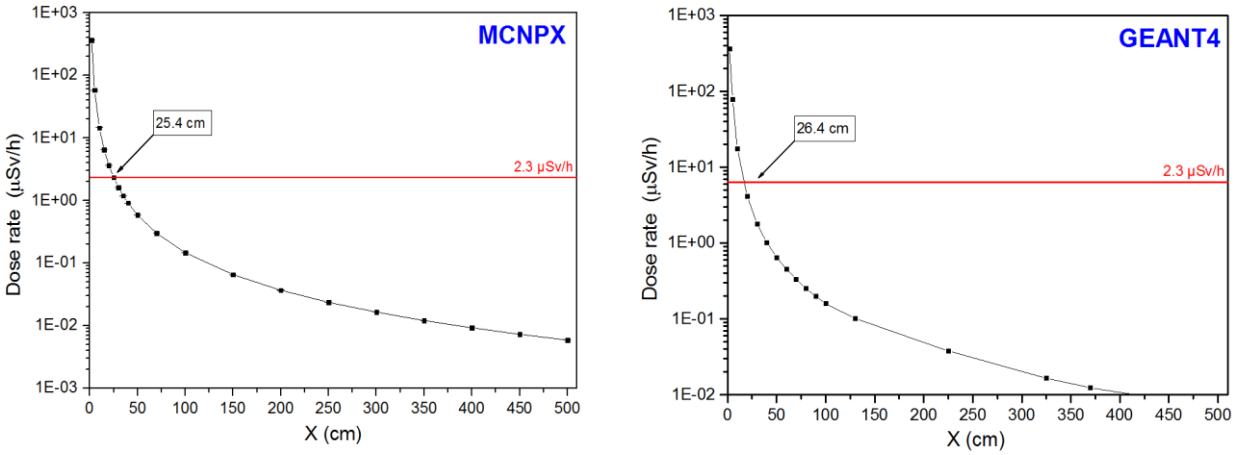

(a) (b)

Figure 5 Dose rate behaviors with the distance in X and Y = Z = 0 for the simplest geometry calculated with MCNPX (a) and GEANT4 (b).

For the simplest case of the SPECT arrangement, when only the mouse phantom and the ^{99m}Tc isotropic source are taken into consideration, figure 5 presents the dose rate distribution along the X-axis calculated by the MCNPX (a) and the Geant4 (b). The photon source is positioned in the coordinate center (0, 0, 0).

As can be seen above, for the MCNPX simulation at distances greater than 25.4 cm of the source, the dose rate considered safe for workers professionally exposed to radiations is achieved. In the case of the simulation performed with the Geant4, this distance is a little higher, 26.4 cm. However, the difference percent between the obtained results is small, only Δ = 3.9%. The results of Geant4 simulation validate those obtained by MCNPX.

In figure 6 are presented the results of the simulations in X axis for the explained before full geometry in the case of SPECT-CT system, but for the ^{99m}Tc source placed in the center of the animal phantom. For the MCNPX results (figure 6 (a)), at the left of the source the considered safe distance is 17.5 cm and at the right 21.3 cm. The difference is mainly given by the presence of the W anode (Z =74) with 2 mm thickness at the left of the source.

The results obtained with the GEANT4 (figure 6 (b)) are also very close to obtained by MCNPX, 18.1 cm at the left and 21.4 cm at the right, which means that the difference percentages with respect to the MCNPX calculations are Δ_{left} = 3.4% and Δ_{right} = 0.5%. Again, the results of the GEANT4 coincide satisfactorily with those of the MCNPX.

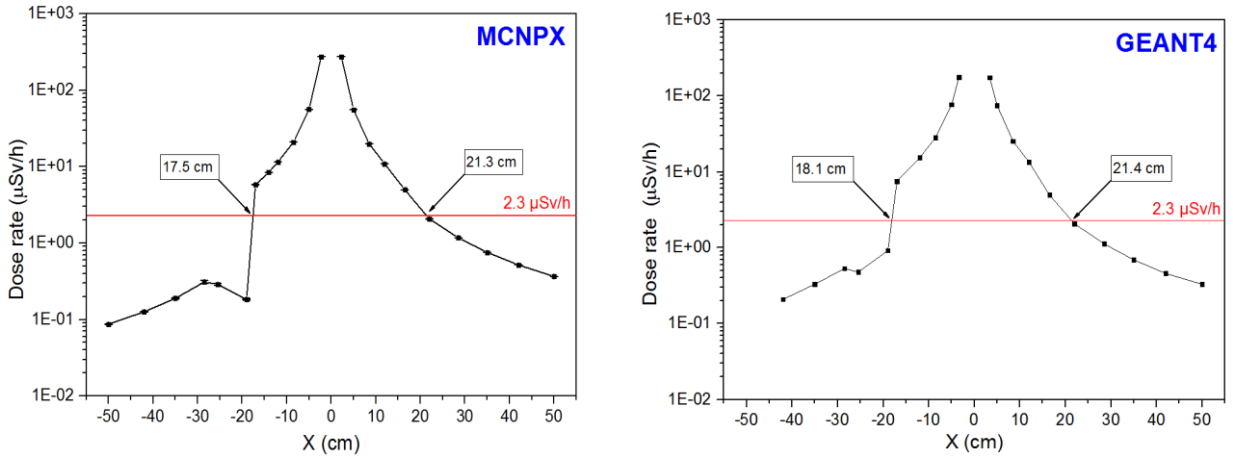

(a) (b)

Figure 6. Dose rate behaviors with the distance in X and Y = Z = 0 for the full geometry calculated with MCNPX (a) and GEANT4 (b).

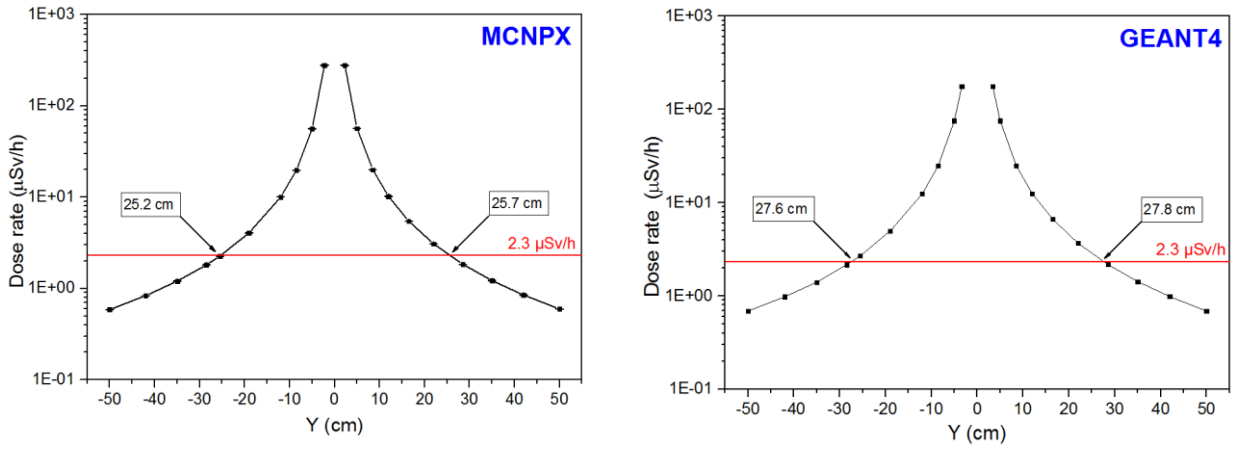

(a) (b)

Figure 7. Dose rate behaviors with the distance in Y and X = Z = 0 for the full geometry calculated with MCNPX (a) and GEANT4 (b).

The results of simulation in the Y axis for this last task using both softwares are presented in figure 7. The safe distance values determined with both the MCNPX and the GEANT4 are once again very similar, which is verified when analyzing the difference percentages that are Δ_{left} = 9.1% and Δ_{righ} = 7.9%. In figures 7 (a) and (b) the values of distances considered safe are shown, highlighting that always the value on the left is slightly lower than that on the right, which is determined by the presence on the left (really the lower part of the arrangement) of the support animal bed.

The distribution of the dose rate along the X and Y axes for the full geometry of the SPECT-CT arrangement, but using the X-ray source explained above is discussed below.

Here it is essential, in order to obtain the dose rate values from the simulation data, to make two important considerations. The first is that only the 1% of accelerated electrons in the tube produce X-ray photons, the rest are lost in heating the target. That is, the efficiency of the X-ray tube is approximately 1% [15-17]. The second one, taking into consideration that the useful X-rays from the tube are emitted towards the target within a cone delimited by an angle of 20º, a simple calculation shows that only the 0.8% of all generated photons can be considered for current experiment.

This allows to estimate the number of photons of interest from the acceleration current in the X-ray tube, which is 350 kV.

The first task in this new calculation was performed for comparative purposes. Instead of the full X-ray emission spectrum, only monoenergetic photons of energy 60, 72, 84 and 120 keV were used (these are average values of the total emission energy of the tube determined according to different criteria). Figure 8 shows the results obtained for these conditions, and demonstrates how with increasing the X-ray source energy, the value of the distance at which the dose rate is safe for the occupationally exposed worker increases. That is why it is important in the simulation to use as source the full spectrum of figure 2.

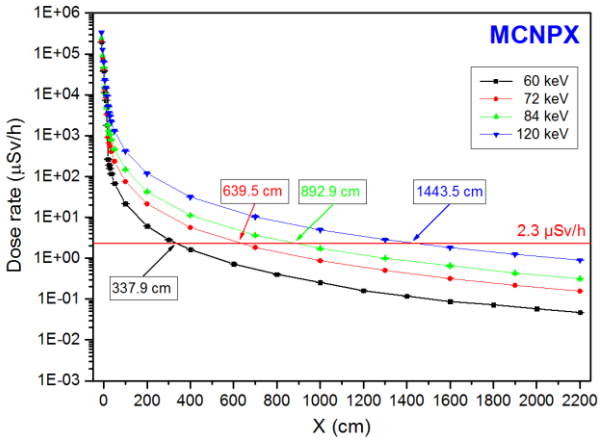

Figure 8. The right branch of the dose rate behaviors with the distance in X and Y = Z = 0 for the full geometry calculated with MCNPX.

In figures 9 and 10 are presented the results of the MCNPX calculations made for the X-ray source using the full W spectrum (120 kV and 350 mA). On the left of these figures the results of the dose rate dependence with the distance for the already explained full geometry are presented. On the right of the figures, the results for the geometry already described, but conventionally adding two 1 cm walls of Al and Pb resulting in an important protective radiation barrier, are presented. Figure 11 shows this new protection introduced.

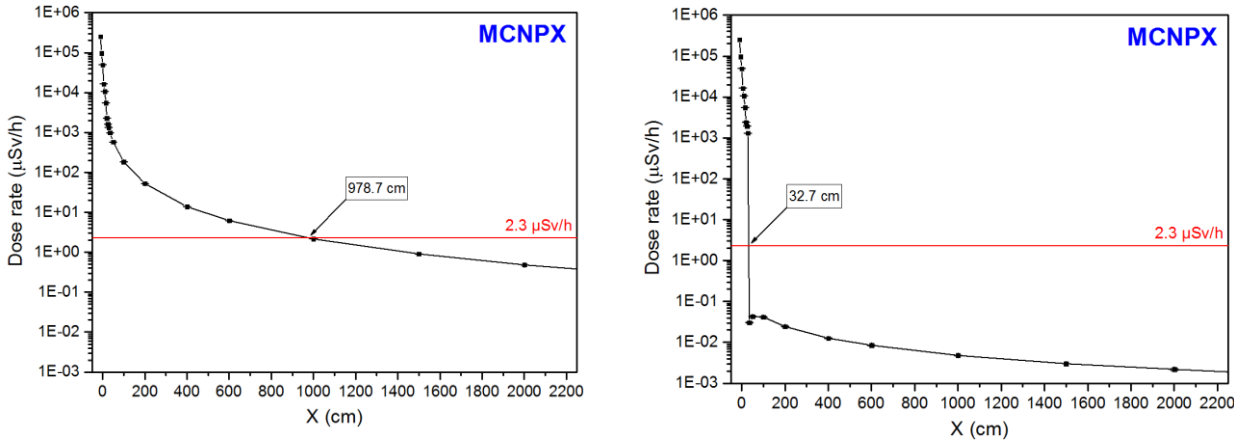

(a) (b)

Figure 9. The right branch of the dose rate behaviors with the distance in X and Y = Z = 0 for the full geometry non considering (a) and considering (b) the Al and Pb protection walls, calculated with MCNPX.

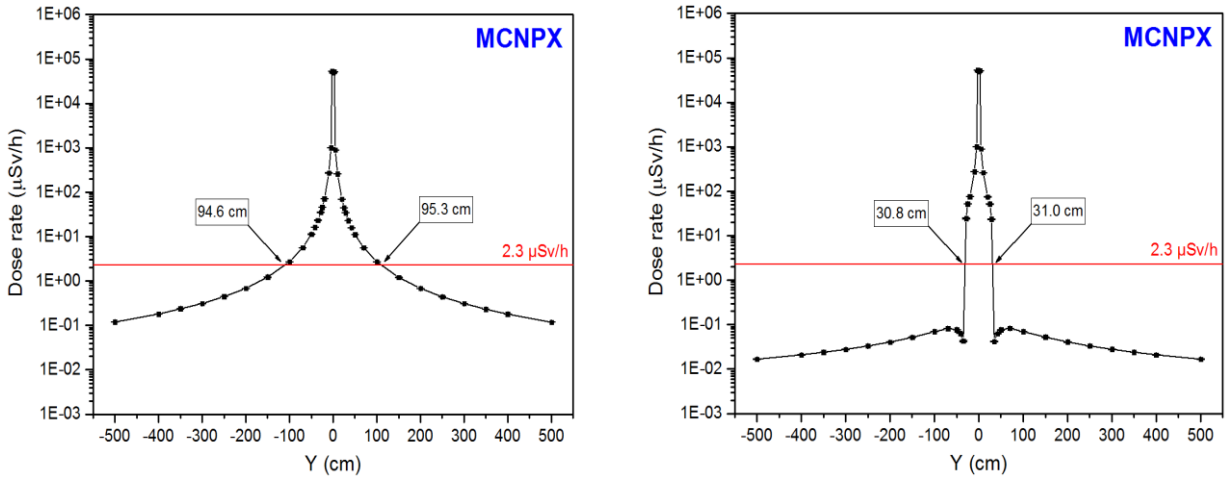

(a) (b)

Figure 10. Dose rate behaviors with the distance in Y and X = Z = 0 for the full geometry non considering (a) and considering (b) the Al and Pb protection walls, calculated with MCNPX.

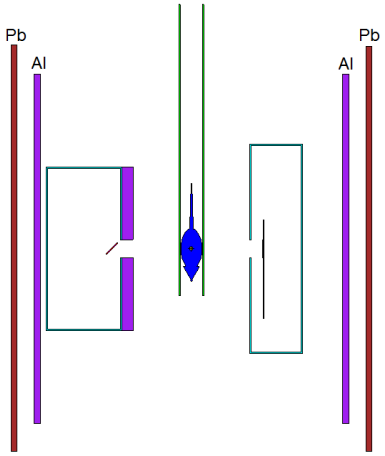

Figure 11. Schema of the studied arrangement with the introduction of protection walls perpendicularly to the X axis.

In figure 9 (a), which shows the result of the calculation on the X axis, it is possible to appreciate that the safe distance from the source in this case is quite large, 978.7 cm. However, when the protection is placed (figure 9 (b)), this value falls to 32.7 cm. This means that the addition of the new Al and Pb walls made the distance for which the dose rate is safe had decreased in 96.7%.

On the Y axis (figure 10), where no protection is added, the values of interest are an order lower than those obtained in X. It is shown that when the protection is added on the X axis, this also significantly influences the results in Y, that fall 67.4%.

These results are of great interest for the work because they allow to made the necessary evaluations leaded to estimate the level of physical protection that is required to be introduced into a real scanning system of this type, so that the radiological safety measures of the personnel are complied with.

Modeling of SPECT phantom using GEANT4.

In order to do a preliminary evaluation of the response of a 1 mm thick CdTe detector to the exposition to the self-constructed SPECT phantom, considering the use of a coded aperture mask, mathematical simulation was used. For this purpose, the Geant4 code was employed.

Figure 12 presents a photograph of the real self-made SPECT phantom. It consists in a plexiglass cylinder, with a density of 1.9 g/cm^3, with 3 cm of length and 1.5 cm of radius. Inside there are two perforations also with a cylindrical shape, parallel to each other (source containers). These internal cylindrical containers are 1.5 cm of length and 2 mm of radius, and their axes are separated by 10 mm. The sources placed in the cylinders are ^{99m}Tc but with different activities; one is 10 times higher other. This is important to evaluate the contrast of the arrangement.

(a) (b)

Figure 12: Top view (a) and front view (b) of the real phantom photography.

The use of "coded aperture mask" seeks the objective of increasing the resolution and efficiency, dismissing the noise in the measurement and image reconstruction processes [18].

In figure 13 (a) is presented the shadowgram on the detector obtained for the case when both sources are at the same distance from the detector, that is, the plane of its axes is parallel to the detector (0^o). In figure 13 (b) the reconstructed image is shown. The obtained

image allows to clearly appreciate the two sources, although the difference in activity cannot be resolved with the naked eye.

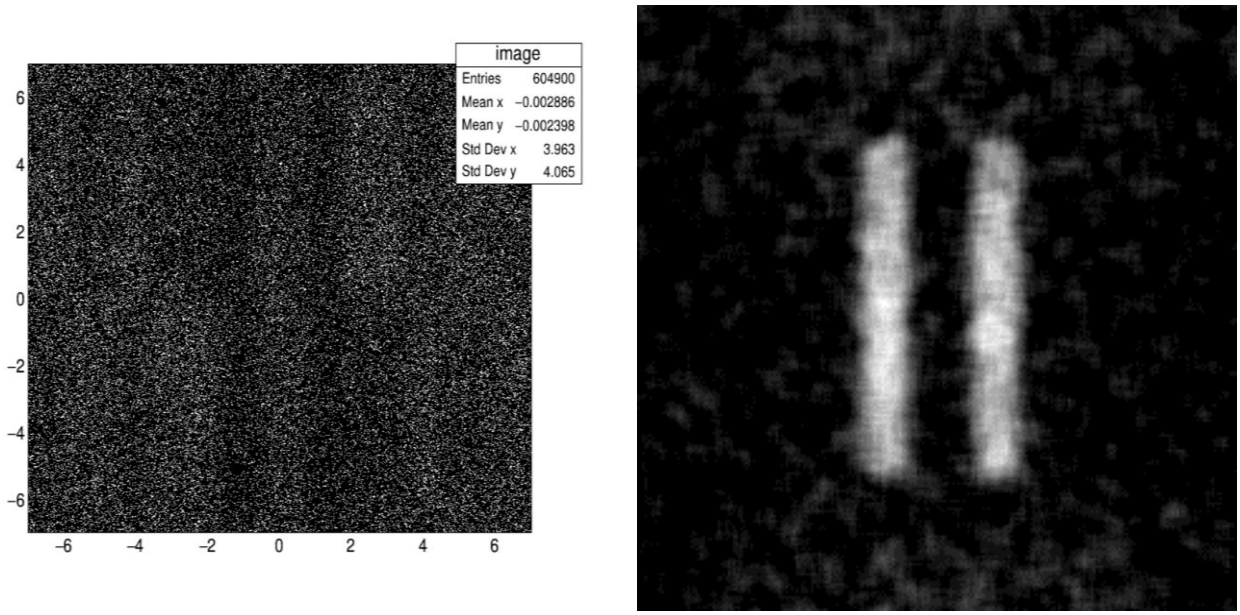

(a) (b)

Figure 13: Shadowgram on the detector for the phantom in 0º (a) and the reconstruction result (b).

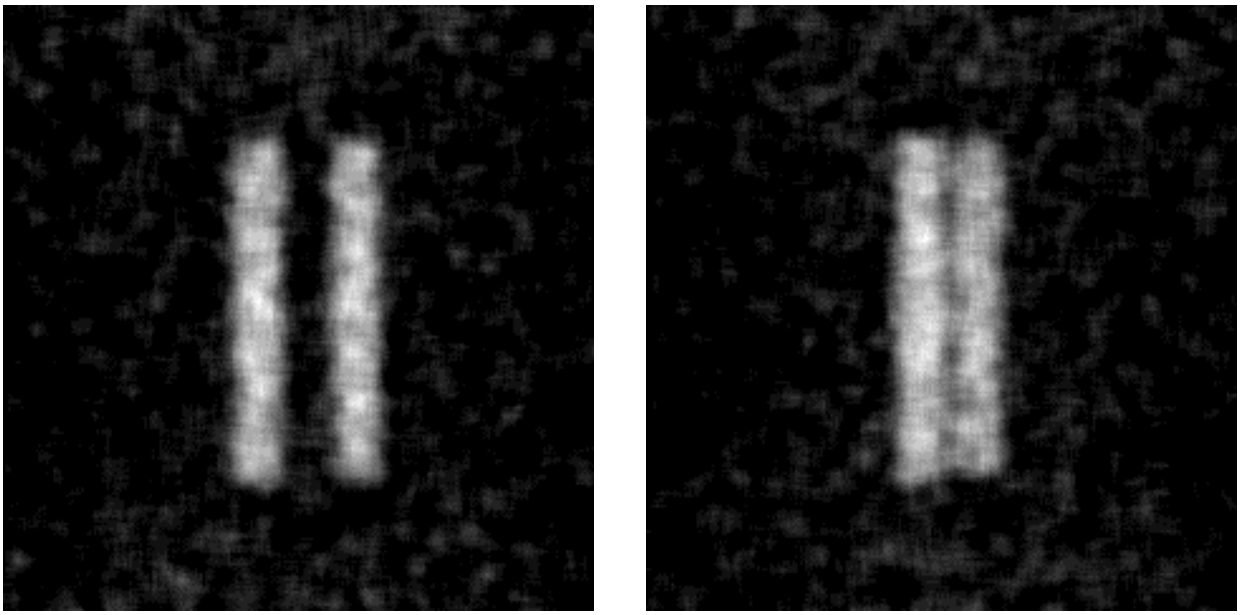

(a) (b)

Figure 14: Imagens obtained for the phantom rotated at 30º (a) and 60º (b).

In order to study the possibility of the detector to resolve the examined phantom sources in different positions, the phantom was rotated and the simulations were made at different angles. In figure 14 some results are presented.

In the both above images the results show that the detector can resolve the separation between the sources, better for the lower angle.

For the case when the phantom is rotated at 60^{o}, the separation of the sources continues to be distinguished although with less resolution. However, the difference in source intensity is better appreciated. In both cases, the source of higher activity is positioned on the left.

In future, it is planned to perform this simulation and image processing for a greater number of angles using a much smaller step.

Conclusions.

In this work, the MCNPX and Geant4 radiation transport simulation codes have been used to study the dose rate distribution in a SPECT-CT scanner system for two types of photon sources, and to obtain the image that a semiconductor detector is capable of registering from a SPECT phantom when a coded aperture mask is used.

The comparison between the results obtained by both codes showed that these were similar, the maximum difference is less than 10%, although on average this was 5%. This result validates the use of either software to perform this task.

For the geometric characteristics of our experiment, the minimum distance considered safe from the point of view of radiation protection for occupationally exposed personnel is 26.4 cm on the X axis and 27.8 cm on the Y axis if the source used is ^{99m}Tc. In the case when using the X-ray source with the W anode, these distances are 978.7 cm on the X axis and 95.3 on the Y axis, but if the system includes an Al and Pb wall protection of the characteristics explained in work then these values fall to 32.7 cm and 31 cm respectively. The inclusion of the walls of Al and Pb in the X axis leads to the safe distance falling between 67.4% and 96.7% with respect to the case when this protection does not exist.

The obtained results in the simulation of the SPECT phantom images show that for the three studied angles before the reconstruction it is possible to appreciate and resolve clearly the two sources. However, the difference in activity only is possible to observe with the naked eye when the phantom rotation angle is 60^{o}.

Recommendations.

It would be interesting to study the distribution of the dose rate in this SPECT-CT system considering the real geometry and dimensions of the walls used as radiological protection in the MARS-CT reference system.

In the near future, it is recommended to perform the simulation related to the phantom SPECT for a greater number of angles using a much smaller step. It is also considered that other types of phantoms should be studied by means of mathematical simulation.

Acknowledgements.

I want to thank the JINR, and in particular the Organizing Committee of the SSP-2019, for allowing me to participate in this program and for all the attention they have given to me during my stay.

I especially want to thank my principal supervisor, Prof. Dr. Antonio Leyva Fabelo, for his unconditional help and support, not only as a supervisor but also as a father. Also, my gratitude for his wife Ileana for all that she has helped me, for her time and dedication.

Also, I would like to acknowledge Prof. Dr. Alexei Zhemchugov and Prof. Vladislav Rozhkov, my second supervisor, for their support and assistance that has been a great help to develop this research.

My special thanks are extended to Dario, Gabriel, and Jose Alejandro for all the help they gave me with the codes and everything else.

References.

1. Rogers D. W., Fifty years of Monte Carlo simulations for medical physics. Phys Med Biol. 51(13), R287-301, (2006). DOI: 10.1088/0031-9155/51/13/R17.
2. Lanconelli N., The importance of Monte Carlo simulations in modeling detectors for Nuclear Medicine, Mathematics and Computers in Simulation, 80(10), 2109-2114, (2010). https://doi.org/10.1016/j.matcom.2010.04.004.
3. Uvat I. B. and Castiglioni I., Monte Carlo simulations in SPET and PET, Q J Nucl Med 46, 48-61, (2002).
4. J. Hsieh, Computed Tomography: Principles, Design, Artifacts, and Recent Advances, Third Edition, PM259, (2015). ISBN: 9781628418255.
5. Wernik M. N. and Aarsvold J. N., Emission Tomography: The Fundamentals of PET and SPECT, Elsevier Academic Press, (2004), ISBN: 0-12-744482-3.
6. Perera A., Torres L. A., Vergara A., et al., SPECT/CT: main applications in nuclear medicine, Nucleus, 62, (2017). ISSN: 2075-5635.
7. Bural G. G., Muthukrishnan A., Oborski M. J., et al., Improved Benefit of SPECT/CT Compared to SPECT Alone for the Accurate Localization of Endocrine and Neuroendocrine Tumors, Mol. Imaging Radionucl Ther. 21(3), 91-96, (2012). doi: 10.4274/Mirt.80299.
8. Heather A. J., S ibyll G., Heena P., et al., Advantages of Hybrid SPECT/CT vs SPECT Alone, The Open Medical Imaging Journal, 2, 67-79, (2008). DOI: 10.2174/1874347100802010067.
9. Rubinstein R. Y. and Kroese D. P., Simulation and the Monte Carlo Method, Third ed., John Wiley & Sons Inc., (2017). ISBN: 9781118632383.
10. Hendricks J. S., LA-UR-08-2216, "MCNPX 2.6.0 Extensions", Los Alamos National Laboratory, April 11 (2008).
11. Geant4 Collaboration, Physics Reference Manual, Release 10.4, (2017). https://indico.cern.ch/event/679723/contributions/2792554/attachments/1559217/2454299/PhysicsReferenceManual.pdf.
12. Apostolakis J. and Wright D. H., An Overview of the Geant4 Toolkit, AIP Conference Proceedings 896, 1, (2007). https://doi.org/10.1063/1.2720452.
13. Boone J. M. and Seibert J. A. An accurate method for computer-generating tungsten anode x-ray spectra from 30 to 140 kV. Med Phys. 24(11), 1661-1670, (1997).

14. ICRP, Conversion Coefficients for Radiological Protection Quantities for External Radiation Exposures. ICRP Publication 116, Ann. ICRP 40(2–5). (2010).
15. Diagnostic Radiology Physics: A Handbook for Teachers and Students, Hellenic Association of Medical Physicists, IAEA Reference Number: STI/PUB/1564 (2014). ISBN: 978-92-0-131010-1.
16. David Dowsett, CRC Press, Taylor & Francis, Radiological Sciences Dictionary, Group p. 351 (2009). ISBN: 978-0-340-94167-6.
17. http://www.antonine-education.com/Pages/Physics_5_Options/Medical_Physics/MED 07/med_ phys_7.htm
18. Stephen R. Gottesman and E. E. Fenimore, New family of binary arrays for coded aperture imaging, Applied Optics 28(20), 4344-4352, (1989). DOI: 10.1364/AO.28.004344.